IEEE Access
Multidisciplinary : Rapid Review : Open Access Journal

Received August 2, 2021, accepted August 22, 2021, date of publication August 24, 2021, date of current version September 1, 2021.

Digital Object Identifier 10.1109/ACCESS.2021.3107625

10 Element Sub-6-GHz Multi-Band Double-T Based MIMO Antenna System for 5G Smartphones

NAVEEN JAGLAN[1], (Member, IEEE), SAMIR DEV GUPTA[1], BINOD KUMAR KANAUJIA[2], (Senior Member, IEEE), AND MOHAMMAD S. SHARAWI[3], (Senior Member, IEEE)

[1]Department of Electronics and Communication Engineering, Jaypee University of Information Technology, Solan, Waknaghat, Himachal Pradesh 173234, India
[2]School of Computational and Integrative Sciences, Jawaharlal Nehru University, New Delhi 110067, India
[3]Poly-Grames Research Center, Electrical Engineering Department, Polytechnique Montréal, Montréal, QC H3C 3A7, Canada

Corresponding author: Naveen Jaglan (naveenjaglan1@gmail.com)

ABSTRACT A 10 element multiple input multi output (MIMO)/Diversity antenna system is considered to work in Sub-6 GHz frequency range. The proposed design can work in long term evolution (LTE) band 42(3.4-3.6 GHz), LTE band 43(3.6-3.8 GHz) and LTE band 46(5.15-5.925 GHz). The proposed design consists of 10 identical and highly isolated T-shaped slot antennas fed with T-shaped lines. All three bands have the return loss values (<-6 dB) and total antenna efficiency (>83%) in free space. The peak value of envelope correlation coefficient is 0.06 and the calculated value of ergodic channel capacity is found to be greater than 41bps/Hz in all the bands.The effect of hand grip as well as the presence of battery and LCD screen is investigated. Simulated results are validated via fabrication and measurement of the proposed design.

INDEX TERMS 5G smartphones, slot antenna, MIMO antenna, sub-6 GHz band.

I. INTRODUCTION

The need for 5G smartphones is expected to increase tremendously in the coming years as most of the countries are going towards fifth generation (5G) communication system. Multiple input multiple output (MIMO) antenna [1] design can increase the system capacity and can minimise the influence of multipath fading. In fourth generation (4G) LTE (long term evolution) communications, two element MIMO antenna designs was quite popular [2] and a lot of research has been done on it. Unlike 4G, 5G communications demand better link reliability and higher data rates [3]. The Massive MIMO (m-MIMO) arrangement needs the integration of huge number of antennas at the base station and larger number of antennas at the user terminal. Therefore, this becomes one of the challenges in the realisation of 5G communication systems.

It has been found by various researchers that at least six to eight antennas [4] are required to form m-MIMO links for 5G communications. The value of the ergodic channel capacity for an 8 × 8 MIMO array at 20 dB signal to noise ratio (SNR) in Rayleigh fading channel conditions can attain a maximum value of 46 bps/Hz. This channel capacity value is around four times [5] when compared to the maximum achievable value for a two element MIMO system of 11.4 bps/Hz. Therefore, high data rate requirement of 5G systems is obtained by enhancing the number and efficiency of antenna elements. Although m-MIMO systems can escalate the channel capacity and data throughput, however adding more antenna elements in a very compact space in 5G smartphones is one difficult task. The individual antenna element must be compact in size, properly decoupled and has to be placed meticulously on the phone (PCB or rim). Different antennas in MIMO systems need to be properly field and port decoupled so as to provide uncorrelated channels. To have smooth transition to 5G communication, the 5G smartphones must have some space reserved for 2G/3G/4G MIMO/diversity antennas [6], [7] as well. Frequencies below 6 GHz are termed as sub-6 GHz bands. In various countries research is going on to design efficient MIMO antennas in this band. Several

The associate editor coordinating the review of this manuscript and approving it for publication was Giovanni Angiulli.

This work is licensed under a Creative Commons Attribution 4.0 License. For more information, see https://creativecommons.org/licenses/by/4.0/

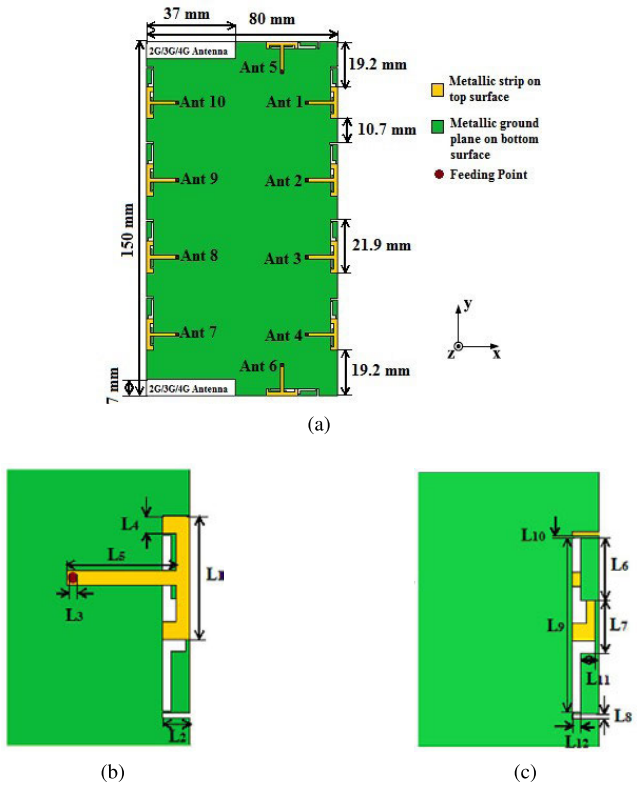

FIGURE 1. (a) Dimensions and geometry of proposed design (b) top view of Ant 1 (c) bottom view of Ant 1.

smartphone antennas designed at sub-6 GHz band have been reported in literature [8]–[14]. In [8] an 8 element antenna array consisting of capacitively coupled element and planar inverted F antenna was proposed at 3.5 GHz. The efficiency of the antenna deteriorates due to the requirement of additional matching circuitry. In [9] an 8 element MIMO antenna system printed on the two long edges of smartphones with capability to integrated with 2G/3G/4G antennas is deliberated at 3.5 GHz. However, the proposed design works only in LTE 42 band. In [10] eight element having combination of C-type fed and L-type monopole slots with orthogonal polarization is proposed. However,the antenna operates only in one band. In [11] eight elements MIMO Antenna array for 5G mobile terminal is investigated. However, the impedance bandwidth of the antenna is only 9.45 %. Moreover, no place is reserved for 2G/3G/4G antennas. In [12] Asymmetrically Mirrored Gap-Coupled Loop Antennas are used to obtain 8 element MIMO antenna array that operates only in LTE 42 band. Nevertheless, the design do not consider a multiband operation that is desired in mobile handsets. In [13], [14] multiband 5G antennas are designed. However,this research is not covering all three bands that is LTE 42,43 and 46. A 12-element antenna array is [15] proposed to work in LTE band 42/43 and LTE band 46. Ergodic channel capacity goes up to 34 bps/Hz for this antenna design. However in the proposed design the placement for 2G/3G/4G antennas are not provided. It is therefore a motivation for antenna designers to design a multiband compact 5G smartphone antenna having proper isolation, better radiation characteristics and excellent MIMO performance. In this work, a 10 element MIMO design functional in sub-6 GHz band is proposed. The projected T-shaped slot antenna fed with a T-shaped microstrip line (hence named double-T) is designed for LTE band 42 (3.4-3.6 GHz), LTE band 43 (3.6-3.8 GHz) and LTE band 46 (5.15-5.925 GHz). The antenna is independent of external decoupling structures thereby giving high total efficiency. Ground plane is having Open ended slots to enhance the isolation among individual antennas. Space is reserved for 2G/3G/4G antennas on the PCB so as to provide a smooth transition to 5G communication system.

II. PROPOSED ANTENNA DESIGN

The detailed geometry and design of the 10 element MIMO antenna design is shown in Fig. 1. The 10 antenna elements named from Ant 1 to Ant 10 and are placed along the sides of substrate.

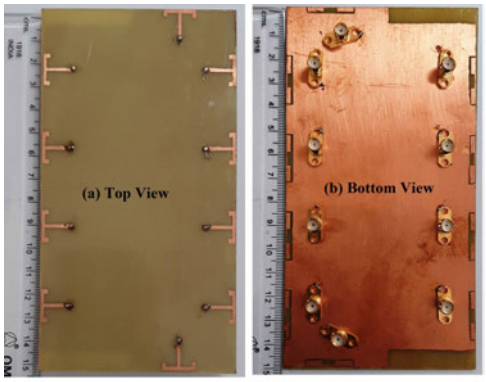

FIGURE 2. Fabricated prototype of the proposed multi band double-T based MIMO antenna system (a) Top view, (b) Bottom view.

The dimensions of the PCB are 150×80 mm which is the standard size of 5.7-inch mobile handset. The dimensions of the proposed antenna as indicated on Fig. 1 are L_1=13.5mm, L_2=3mm, L_3=1.4mm, L_4=2mm, L_5=12mm, L_6=6.6mm, L_7=5.8mm, L_8=0.5mm, L_9=19.3 mm, L_{10}=0.1mm, L_{11}=1.5mm and L_{12}=1mm. The recommended design is fabricated using an FR4 substrate with relative permittivity of 4.4 and loss tangent of 0.002. Double T-shaped antennas Ant 1 to Ant 4 are located on the larger edge and Ant 5 is used on the shorter edge of the smartphone. Ants 7 to Ant 10 are mirror images of Ant 1 to Ant 4 while Ant 6 is mirror image of Ant 5. The space for 2G/3G/4G MIMO antennas is also reserved on the PCB.

Individual antenna elements are fed with 50-ohm T-shaped microstrip feedline that is linked to ground plane through SMA connector. As per the boundary conditions which states that the tangential component of the electric field is zero on perfect conductor, the electric field vanishes at the ends of the slots. The amplitude distribution of the electric fields for both the resonant modes of the slot antenna needs to be different. To make the design more flexible, frequency ratio of both the resonant modes can be adjusted using branched slot approach

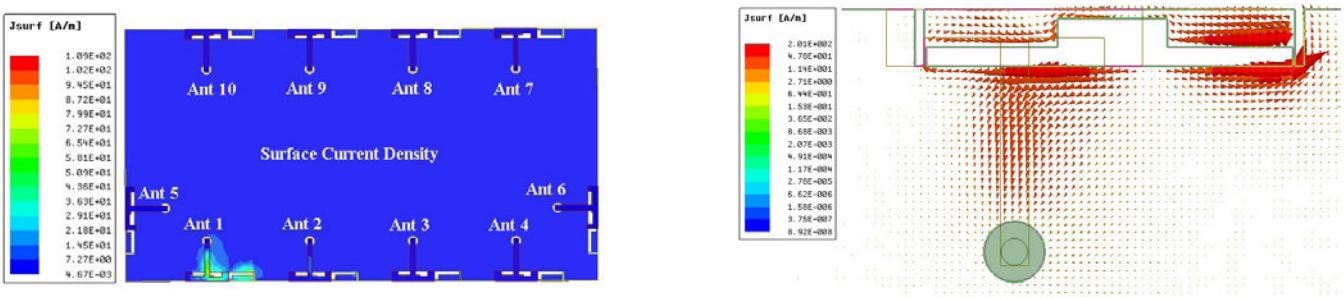

(a) (b)

FIGURE 3. (a) surface electric current on antenna ground plane when Ant 1 is excited at 5.5 GHz, (b) surface current distribution on Ant 10 at 5.5 GHz.

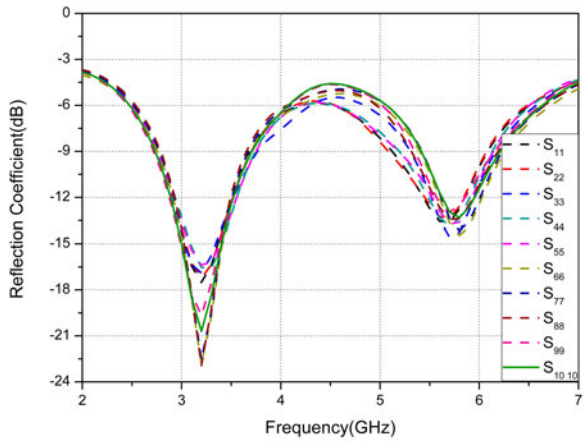

FIGURE 4. simulated reflection coefficient variation with frequency for Ant 1 to Ant 10.

as discussed in [16]. T-shaped feeding structure are designed for the antenna element, which makes it possess a wide bandwidth with dual resonance modes, required radiation characteristics, and comparatively high gain. The slot radiator has dimensions of $3 \times 19.3\ mm^2$ ($0.03\lambda \times 0.22\lambda$), with λ as free space wavelength calculated at 3.4 GHz. Open ended slots are employed in antenna ground to minimise mutual coupling effects. Internal decoupling mechanism is used because external decoupling elements can degrade the efficiency of the proposed design. The arrangement of antenna elements placed on longer edge of smartphones is kept at a distance of 10.7 mm. The proposed double-T antenna can form 10×10 MIMO antenna array in all the operating bands. Therefore, this antenna can be used in future smartphones that will have massive MIMO capabilities not limited to conventional LTE bands 42 and 43 but even in LTE band 46. In Fig. 2, top and bottom side views of proposed fabricated MIMO antenna array is given. The proposed design is simulated, fabricated and tested to validate the obtained results. HFSS version 17 is used to simulate the results. Agilent^{TM} Network Analyzer PNA-L series is used to measure S-parameters. The total efficiency and radiation characteristics of the presented design are tested using microwave shielded anechoic chamber.The current distribution on the ground plane of antenna is shown to understand the mutual coupling effect. In Fig. 3a the current distribution on Ant 1 is shown at 5.5 GHz. It can be observed from the figure that when one antenna element is excited, the current does not spread to the adjacent antenna elements. The open-ended decoupling helps in minimising the coupling between antenna elements.In Fig. 3b surface current distribution is shown on the ground plane of Ant 10 at 5.5 GHz. It can be observed that maximum current flows around the edges of slot. Non-uniform vector current distribution is shown where the length of the arrow also denotes the strength of the current. The current is minimum in the centre of the slot and increases along the sides. The current is maximum on the edges of the slot and voltage is minimum on edges of slot. The currents are flowing in opposite direction along the edges thereby cancelling the net effect. Voltage will be maximum in the centre of the slot and thereby corresponding electric field is added in phase and is responsible for radiations.

III. RESULTS AND DISCUSSION

A. S-PARAMETERS,RADIATION PATTERNS AND ANTENNA EFFICIENCY

Fig. 4 depicts the simulated reflection coefficient variation with frequency for Ant 1 to Ant 10. It can be analysed that the reflection coefficient is quite better than -6 dB (3:1 voltage standing wave ratio, VSWR) for all the operating bands. Fig. 5 presents measured reflection coefficients values for different antenna elements. Fig. 5a shows the variation of measured reflection coefficients variation with frequency for Ant 1 to Ant 5. Fig. 5b represents variation of measured reflection coefficient values with frequency for Ant 6 to Ant 10. It can be seen throughout the paper that simulated and tested outputs are in close agreement. The proposed antenna have exhibited desirable measured 6-dB impedance bandwidths (3:1 VSWR) of 5.71% (3400–3600 MHz), 5.40% (3600–3800 MHz) and 14% (5150–5925 MHz). Fig. 6a shows the simulated values of coupling variations for various combinations of antenna elements. Fig. 6b shows the measured values of coupling among various antenna elements. It can be concluded that the magnitude of isolation has a value of more than 20 dB over all three operating bands of different antenna pairs.

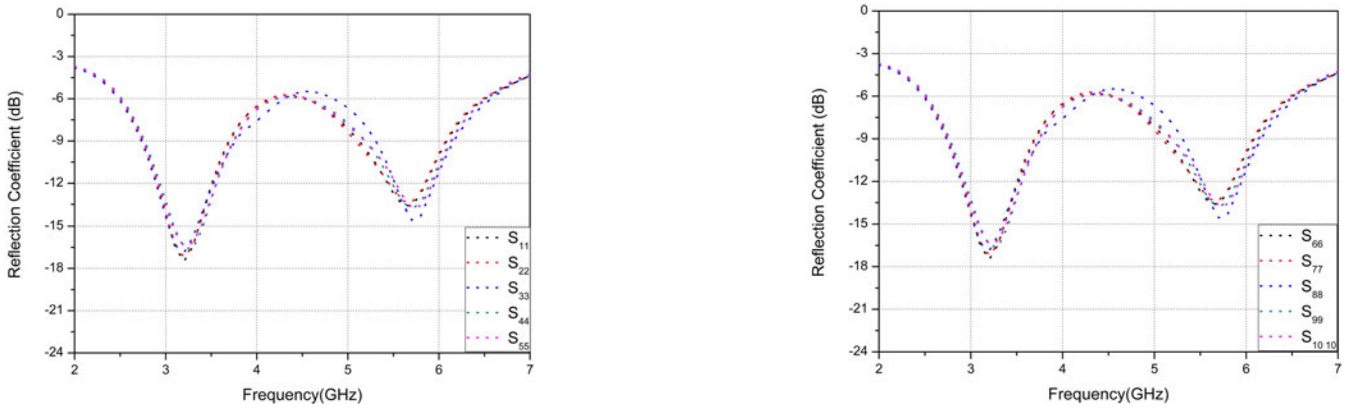

(a) (b)

FIGURE 5. Variation of measured reflection coefficient values with frequency (a) Ant 1 to Ant 5, (b) Ant 6 to Ant 10.

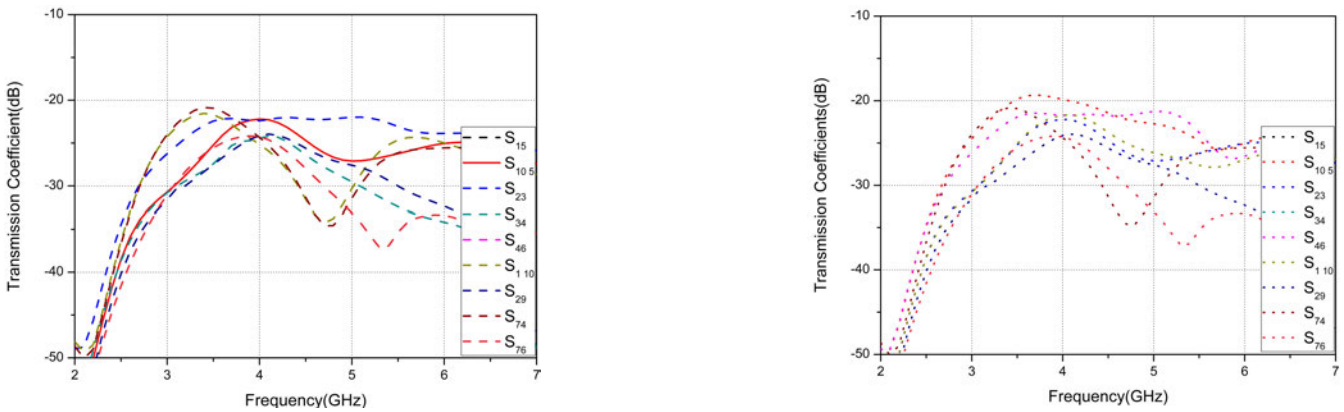

(a) (b)

FIGURE 6. (a) Simulated values of coupling among different antenna pairs, (b) Measured values of coupling among different antenna pairs.

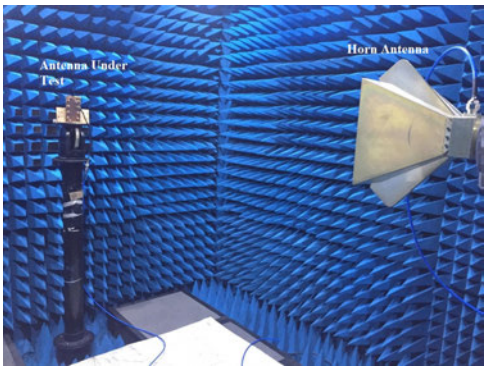

FIGURE 7. Testing setup of the proposed antenna in an anechoic chamber.

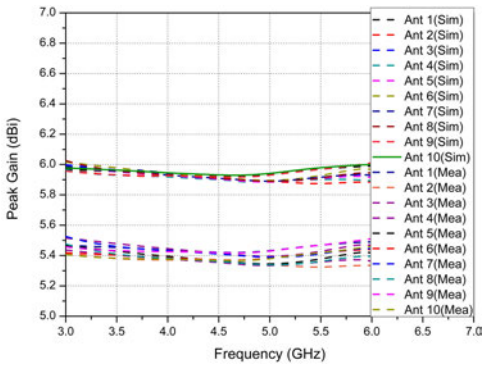

FIGURE 8. Simulated (Sim) and Measured (Mea) peak gain values of Ant 1 to Ant 10.

Open ended slots are utilised on the antenna ground plane to minimise coupling among various antenna elements. Open ended slots act like band stop filter. The frequency of operation for the open-ended slots can be calculated using slot length. An equivalent circuit can be obtained which exhibits resonance at the operating frequency of the antenna. The slot can be considered as a circuit element that is to be matched for resonance.

These equivalent circuits models are appropriate for narrow slots as considered in this work. For a wide slot, in the equivalent circuit one has to consider additional parasitic effects. The coupling coefficients among adjacent antenna elements are calculated and optimised with the help of slot length. Fig. 7 represents the measurement setup of the proposed antenna in a microwave shielded far field anechoic

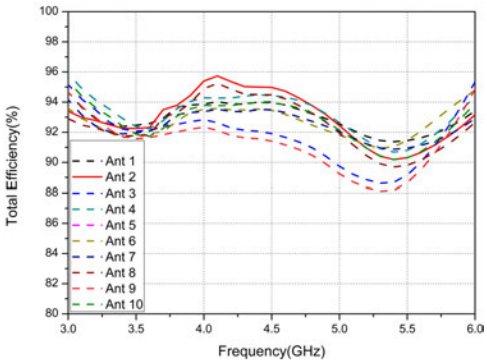

FIGURE 9. Variation of simulated values of antenna efficiency for different antenna elements.

chamber. Fig. 8 shows that simulated gain of individual antenna elements is greater than 5.9 dBi and the measured value of gain for antenna elements are greater than 5.3 dBi.

Fig 9 represents simulated radiation efficiency values for Ant 1 to Ant 10. The measured radiation efficiency values for Ant 1 to Ant 5 are given in Fig. 10a. Fig. 10b represents the measured radiation efficiency values for Ant 6 to Ant 10. Both simulated and measured radiation efficiency values are found to be greater than 83%. The simulated and tested gain patterns of different antenna elements in xoy plane are shown in fig. 11. Fig. 11a represents the theta and phi polarized gain pattern for Ant 1 at 3.5 GHz. Fig. 11b shows the radiation characteristics of Ant 1 at 5.5 GHz. Fig. 11c presents the simulated and measured gain pattern for Ant 5 at 3.5 GHz. Fig. 11d shows the pattern of Ant 5 at 5.5 GHz. Fig. 11e depicts the gain pattern for Ant 8 at 3.5 GHz. Fig. 11f indicates the radiation pattern of Ant 8 at 5.5 GHz. Simulated and measured 2D radiation patterns of various antenna elements are found to be in close agreement.

B. DIVERSITY AND MULTIPLEXING PERFORMANCE

MIMO antennas are mainly based on diversity and multiplexing capabilities of antenna elements. It becomes extremely important to scrutinize multiplexing and diversity performance of MIMO antenna array besides s-parameters and radiation characteristics. Envelope Correlation Coefficient (ECC) is the most significant characteristics to estimate and validate the diversity characteristics of proposed design. If adjacent antenna elements are having ECC value of less than 0.5 then they are considered as highly uncorrelated. If ECC value increases beyond 0.5 then there will be correlation between the antenna elements and radiation performance of the antenna deteriorates. The Envelope correlation coefficients (ρ^2) [17], [18] is calculated from 3D far field radiation patterns for each antenna pairs.

The environment is assumed to be isotropic having uniform distribution of horizontal and vertical components of incoming waves. Isotropic environment is widely adopted in multipath scenarios where MIMO systems are employed. It can be realized from Fig. 12a that simulated ECC value is less than 0.06 over whole functioning frequency range. Fig. 12b shows the measured values of ECC for different antenna elements which are less than 0.06 over the entire operating frequencies of the proposed design. Ergodic channel capacity of the proposed double-T based MIMO antenna array is computed by considering the antenna in independent and identically distributed Rayleigh fading environment [19] with SNR of 20 dB. While calculating ergodic channel capacity it is also supposed that equal power is given to all the antenna elements. Fig. 13 represents the calculated value of ergodic channel capacity of the designed antenna is around 41 bps/Hz at the frequency of operation. The peak value of ergodic channel capacity for a 10 × 10 antenna array can reach upto 57.5 bps/Hz. For a 2 × 2 antenna array peak value of ergodic channel capacity is 11.5 bps/Hz. Therefore, it can be concluded that 10 × 10 antenna array has advantages in data throughput over 2 × 2 antenna array.

C. COMPARISON WITH OTHER 5G SMARTPHONE ANTENNAS

Table 1 gives the comparison of proposed antenna with different state of the art 5G antennas. The proposed antenna can work in LTE band 42(3.4-3.6GHz), LTE band 43(3.6-3.8GHz) and LTE band 46(5.15-5.925 GHz). The proposed antenna design also has the space available for 2G/3G/4G antennas and hence can be used for 2G/3G/4G communication. The authors in [20]–[22] proposed similar designs however the designs do not have space reserved for 2G/3G/4G antennas. Moreover, isolation among antenna elements, total efficiency and peak channel capacity of the designs is less as compared to the design proposed in this paper. The antenna designed in [23] has space reserved for 2G/3G/4G antenna elements but having lesser values of channel capacity, isolation among antenna elements and total efficiency. The proposed antenna in [24] operates only in LTE band 42 and 43 and has a impedance bandwidth of only 11.11 %. In [25], [26] 4 × 4 MIMO antenna array is designed that will have lesser peak channel capacity values when compared to the proposed antenna. In [27], [28] edge side-frames with thickness upto 7 mm are used to design the antenna elements. The proposed design in this paper achieves better values of isolation, ECC, total efficiency and peak channel capacity without using edge side-frames. Therefore the proposed design can be considered suitable for multi-band applications in thin 5G smartphones.

D. EFFECT OF USER HAND

Effects of user hand on the proposed 5G smartphone antenna is also shown and analysed in this section. Fig. 14a shows the configuration of hand with proposed antenna design in Single Hand Mode (SHM). Fig. 14b shows the proposed antenna design in Double Hand Mode (DHM). Human head impact is not analysed this research as the focus of sub-6 GHz frequency band is on data transmission mode rather than talk mode. In SHM Ant 1, Ant 2, Ant 5 and Ant 9 are blocked by

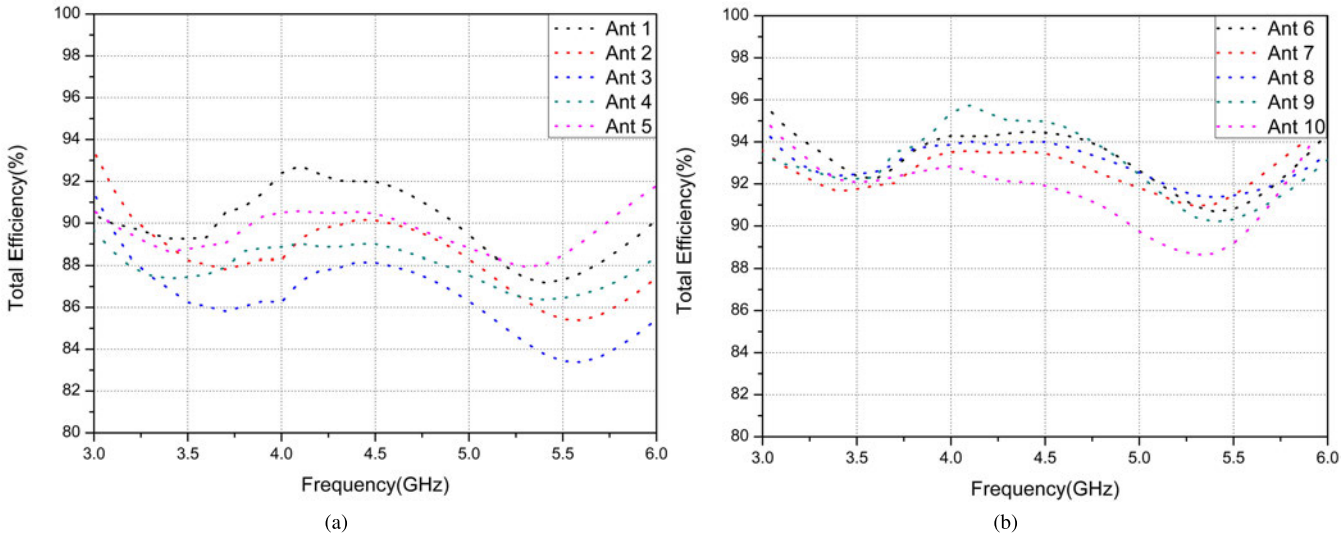

FIGURE 10. Measured antenna efficiency values for various antenna elements (a) Ant 1 to Ant 5, (b) Ant 6 to Ant 10.

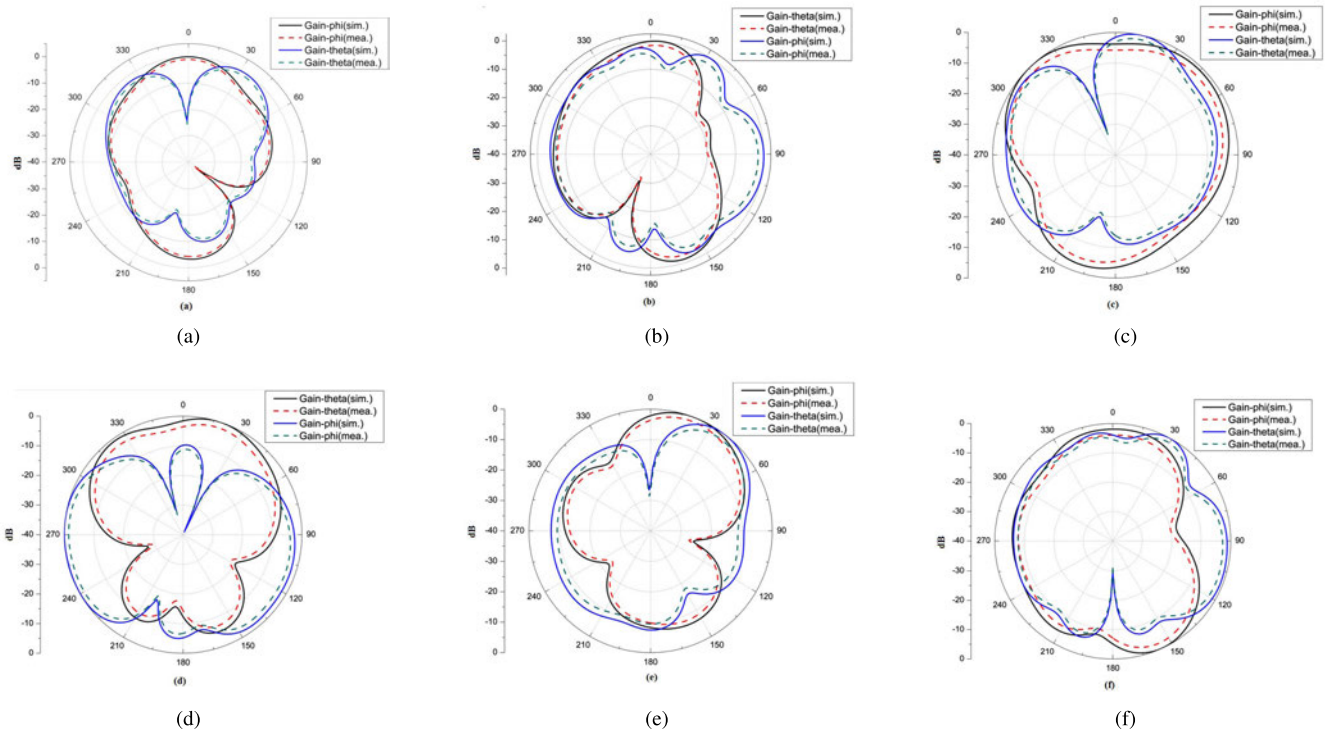

FIGURE 11. Simulated and measured radiation characteristics of (a) Ant 1 at 3.5 GHz, (b) Ant 1 at 5.5 GHz, (c) Ant 5 at 3.5 GHz, (d) Ant 5 at 5.5 GHz, (e) Ant 8 at 3.5 GHz and (f) Ant 8 at 5.5 GHz.

user hand and hence corresponding antennas shows reduced total efficiency values. Fig. 15a shows the reduced efficiencies values for Ant 1, Ant 2 and Ant 5 in SHM. Fig. 15b shows the reduced total efficiency for Ant 9 as compared to other antennas because of SHM configuration. Ant 5 and Ant 6 are blocked by user hand in DHM and hence provides reduced efficiencies in DHM. Fig. 16a represents reduced antenna efficiency values for Ant 5 and Fig. 16b shows the reduced efficiency for Ant 6. Ergodic channel capacity of the proposed design is also calculated in SHM and DHM. It can be seen that due to the hand effect, few antenna elements are blocked by the hand of user and thereby significantly effecting the ergodic channel capacity values. It can be observed from Fig. 17 that the calculated values of ergodic channel capacity reach upto 30.5 bps/Hz and 20 bps/Hz for SHM and DHM respectively.

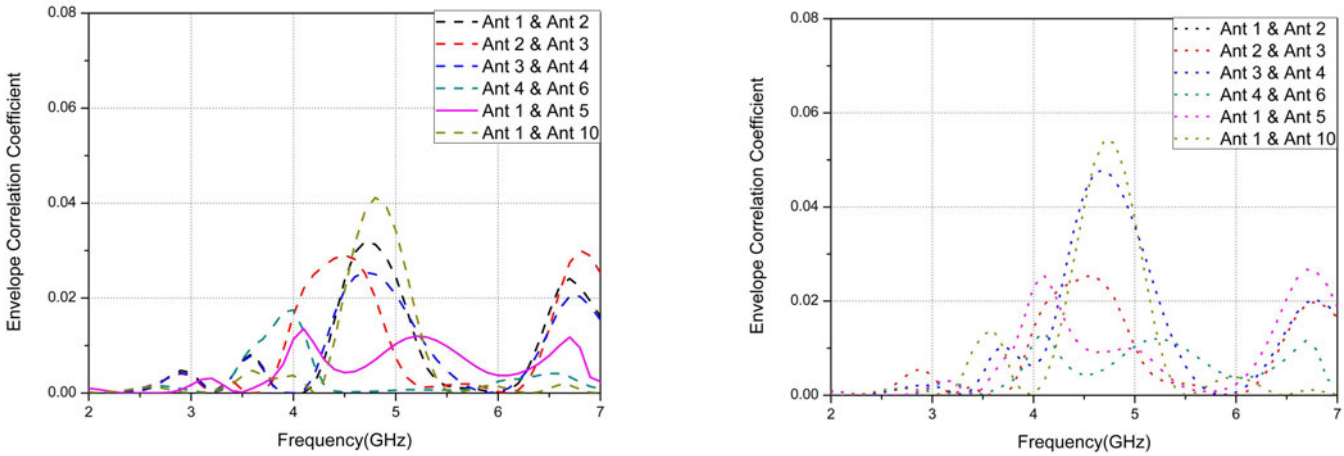

FIGURE 12. (a) Simulated envelope correlation coefficient values for different antenna pairs, (b) Measured envelope correlation coefficient values for different antenna pairs.

TABLE 1. Performance comparison of various state of the art 5G antennas.

References	Bandwidth (GHz)	Isolation (dB)	ECC	Total Efficiency (%)	Radiator size in (λ^3)	Impedance Bandwidth (%)	Peak Channel Capacity (bps/Hz,20dB SNR)
Proposed	3.4-3.8, 5.15-5.925 (-6 dB)	>20	<0.06	83-93	0.03 × 0.22 × 0.02	25.11	41 (10×10).
[14]	3.4-3.6, 5.15-5.925 (-6 dB)	>12	<0.1	>50	0.17 × 0.05 × 0.01	19.71	38.8 (8×8).
[20]	3.4-3.6, 4.8-5.1 (-6 dB)	>11.5	<0.1	40-85	0.17 × 0.03 × 0.01	11.77	38.5 (8×8).
[21]	2.496-2.69,3.4-3.8 (-6 dB)	>10.5	<0.2	44-66	0.02 × 0.17 × 0.01	18.59	38.3 (8×8).
[22]	3.35-3.82,4.79-6.2 (-6 dB)	>10.5	<0.12	>43	0.17 × 0.03 × 0.01	41.77	37.6 (8×8).
[23]	3.4-3.8,5.15-5.925 (-6 dB)	>12	<0.15	41-79	0.13 × 0.04 × 0.01	25.11	29.5 (6×6).
[24]	3.4-3.6,3.6-3.8 (-10 dB)	>20	<0.01	>87	0.11 × 0.04 × 0.02	11.11	81 (18×18).
[25]	3.4-3.6, 4.8-5 (-10 dB)	>16.5	<0.01	82-85	0.16 × 0.07 × 0.01	9.79	Not mentioned (4×4).
[26]	3.3-3.8, 4.8-5, 5.15–5.35, 5.725–5.85 (-10 dB).	>15	<0.02	>70	0.16 × 0.07 × 0.01	24.02	Not mentioned (4×4).
[27]	3.1-3.85, 4.8-6 (-10 dB)	>17	<0.06	65-71	0.20 × 0.05 × 0.01	36.17	39 (8×8).
[28]	3.3-4.2,4.8-5.0 (-6 dB)	>10	<0.12	53.8-79.1	0.21 × 0.07 × 0.01	28.10	39.5 (8×8).

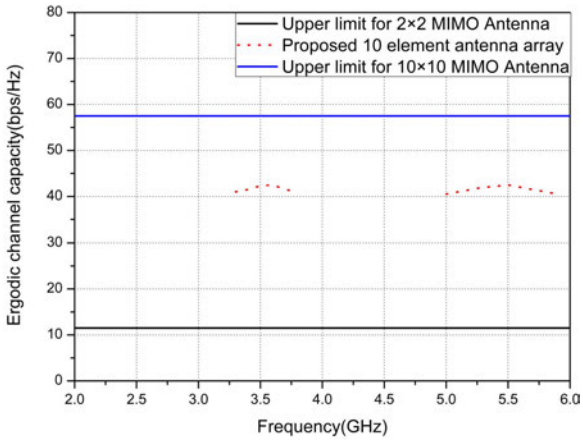

FIGURE 13. Calculated values of ergodic channel capacity for proposed double-T based antenna.

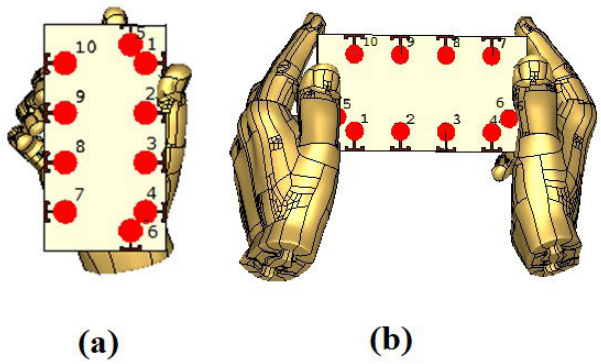

FIGURE 14. Handheld smartphone representation in (a) Single Hand Mode (SHM),(b) Double Hand Mode (DHM).

E. EFFECT OF SMARTPHONE BATTERY

The proposed design is investigated with a metal piece of size 118mm × 40mm × 4mm. This metal block is assumed equivalent to a battery, placed on the front surface of PCB and connected to ground plane with 20 shorting pins. The configuration of the proposed design with battery is shown in Fig. 18. Fig. 19 shows the variations of reflection

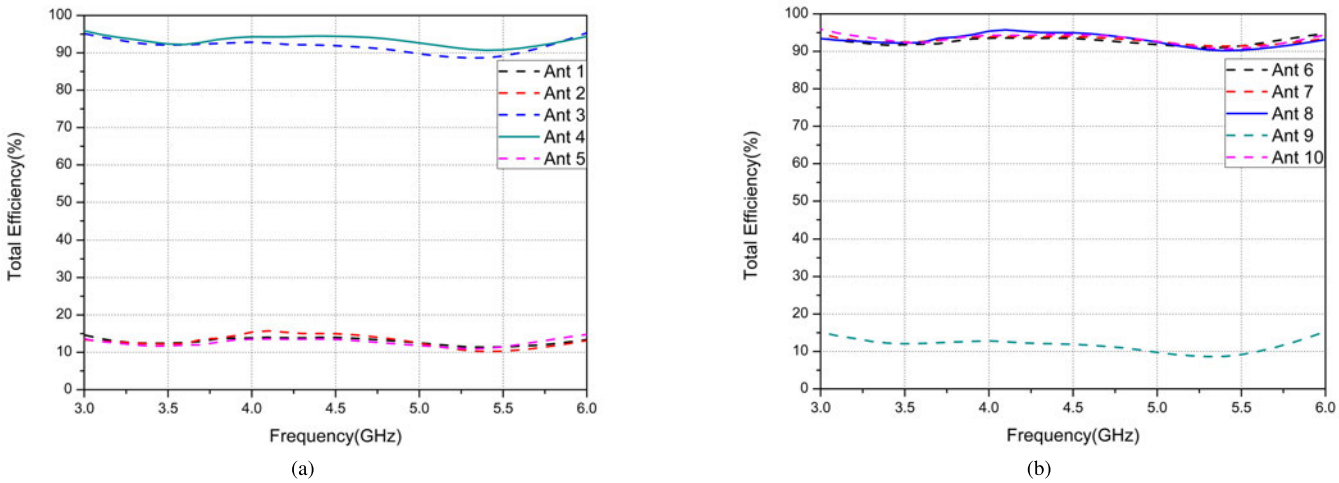

FIGURE 15. (a) Simulated antenna efficiency values for Ant 1 to Ant 5 in SHM, (b) Simulated antenna efficiency values for Ant 6 to Ant 10 in SHM.

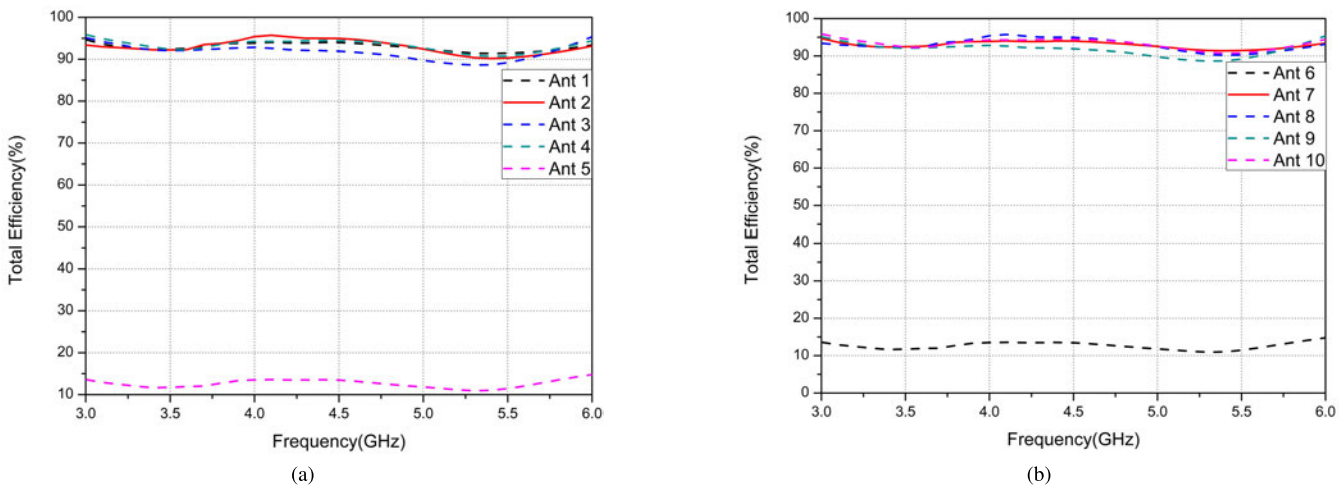

FIGURE 16. (a) Simulated antenna efficiency values for Ant 1 to Ant 5 in DHM, (b) Simulated antenna efficiency values for Ant 6 to Ant 10 in DHM.

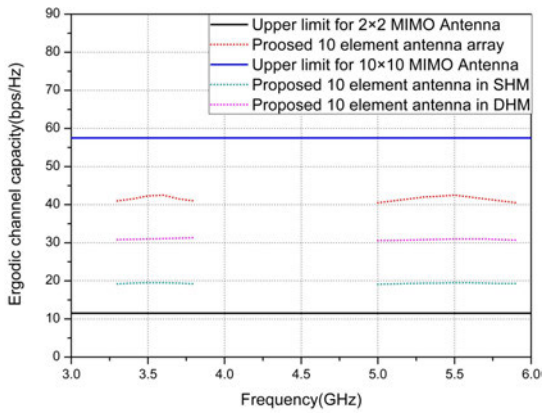

FIGURE 17. Ergodic channel capacity calculation from measured values with hand effects.

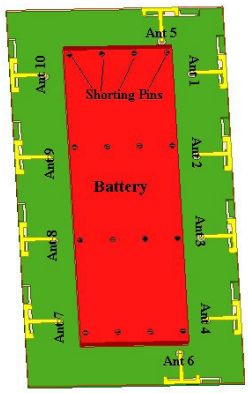

FIGURE 18. Simulation model of the proposed antenna considering the effect of battery.

coefficients with frequency for battery integrated smartphone MIMO antenna designs. It can be seen from the figure that negligible deviations are observed in s-parameters. Fig. 20 shows the total efficiencies of the proposed antenna elements, a minor effect can be observed on efficiency values due to addition of battery.

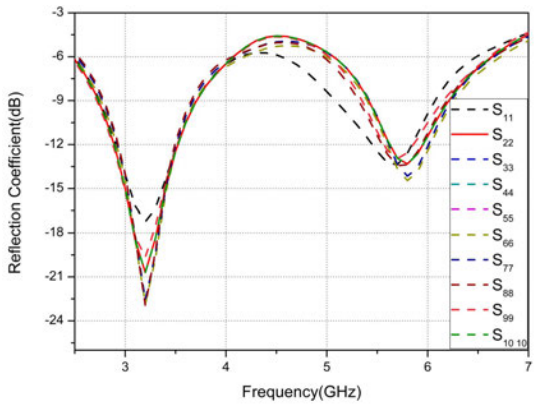

FIGURE 19. Simulated values of reflection coefficients considering the effect of battery.

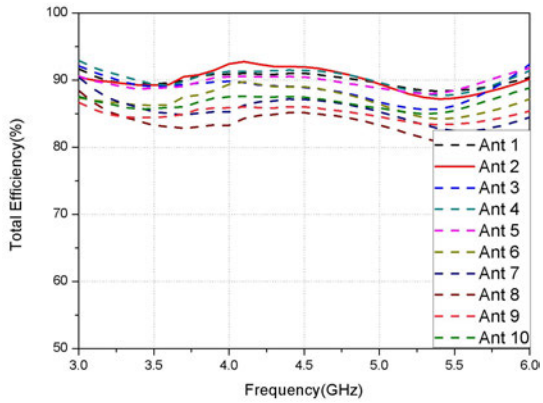

FIGURE 20. Simulated values of antenna efficiency considering the effect of battery.

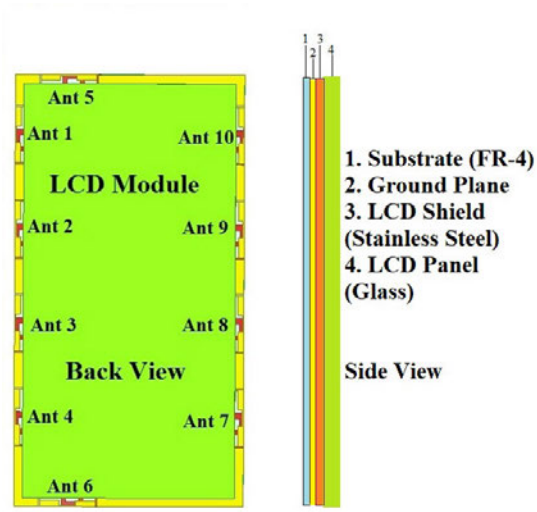

FIGURE 21. Simulation model of proposed antenna with LCD module.

F. EFFECT OF LCD MODULE

Fig. 21 represents the model of proposed antenna array integrated with liquid crystal display (LCD) that is used in simulation. The LCD module is made up of combination of

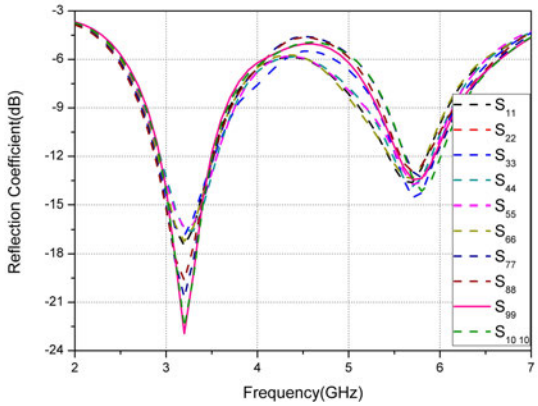

FIGURE 22. Reflection coefficient variations of proposed antenna considering effect of LCD module.

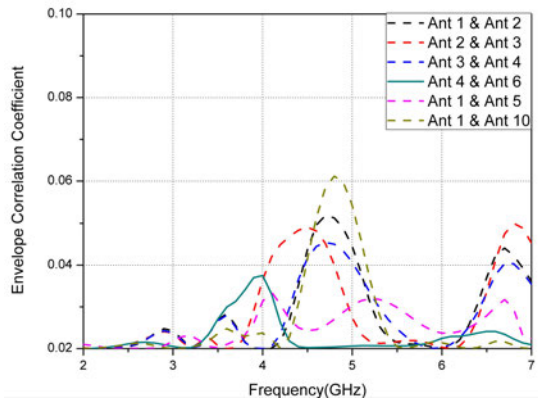

FIGURE 23. Simulated ECC values among different antenna elements considering effect of LCD module.

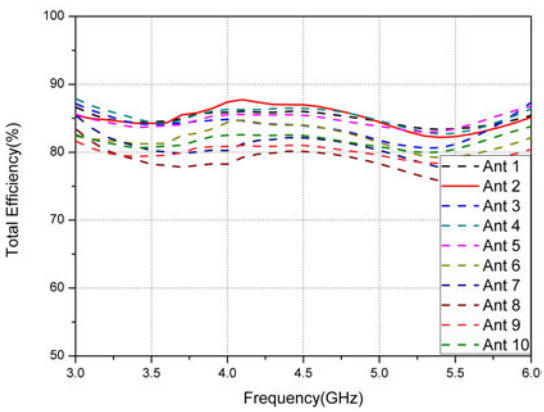

FIGURE 24. Simulated antenna efficiency values with LCD module.

LCD shield and LCD panel. The dimensions of both LCD shield and LCD panel are 144mm × 74mm × 1mm. LCD shield is manufactured with stainless steel and is attached to the ground plane. LCD panel is attached to LCD shield and is made up of glass with relative permittivity of 7 and loss tangent of 0.02. The small size of the proposed antenna provides advantage as LCD modules extends upto the slot radiators and tends to interfere. Minimum variations

are observed on s-parameters, efficiency and ECC by the addition of the LCD module. The reflection coefficient of proposed LCD integrated antenna design is shown in Fig. 22.

It can be seen from the figure that even after addition of LCD module the reflection coefficient is better than -6dB (3:1 Voltage standing wave ratio, VSWR) in LTE 42, LTE 43 and LTE 46 bands. The simulated value of ECC is shown in Fig. 23. It can be seen that ECC is less than 0.07 over the operating frequency of the proposed antenna. The simulated value of antenna efficiency with frequency is plotted in Fig. 24. It can be seen that even after addition of LCD module the efficiency values are greater than 75%.

IV. CONCLUSION

In this paper 10 element array operating at LTE band 42(3.4-3.6GHz), LTE band 46(5.15-5.925 GHz), and LTE band 43(3.6-3.8GHz) for future 5G smartphones is presented that is based on novel double-T elements. The proposed designs have space available for 2G/3G/4G antennas and hence can also be compatible with 2G/3G/4G communications. No extra decoupling structures are added to diminish mutual coupling among individual antenna elements. The design obtains a good isolation of more than 20 dB, ECC value of less than 0.06 and efficiency of greater than 83%. The ergodic channel capacity of the proposed antenna is 41 bps/Hz at 20 dB SNR. It can be established that projected design can be used as a favourable applicant for future 5G smartphones.

REFERENCES

[1] M. Agiwal, A. Roy, and N. Saxena, "Next generation 5G wireless networks: A comprehensive survey," *IEEE Commun. Surveys Tuts.*, vol. 18, no. 3, pp. 1617–1655, 3rd Quart., 2016.

[2] M. Stanley, Y. Huang, H. Wang, H. Zhou, Z. Tian, and Q. Xu, "A novel reconfigurable metal rim integrated open slot antenna for octa-band smartphone applications," *IEEE Trans. Antennas Propag.*, vol. 65, no. 7, pp. 3352–3363, Jul. 2017.

[3] J. G. Andrews, S. Buzzi, W. Choi, S. V. Hanly, A. Lozano, A. C. Soong, and C. J. Zhang, "What will 5G be?" *IEEE J. Sel. Areas Commun.*, vol. 32, no. 6, pp. 1065–1082, Jun. 2014.

[4] R. Hussain, A. T. Alreshaid, S. K. Podilchak, and M. S. Sharawi, "Compact 4G MIMO antenna integrated with a 5G array for current and future mobile handsets," *IET Microw., Antennas Propag.*, vol. 11, no. 2, pp. 271–279, 2017.

[5] H. Li, Z. T. Miers, and B. K. Lau, "Design of orthogonal MIMO handset antennas based on characteristic mode manipulation at frequency bands below 1 GHz," *IEEE Trans. Antennas Propag.*, vol. 62, no. 5, pp. 2756–2766, May 2014.

[6] Y. Li, C.-Y.-D. Sim, Y. Luo, and G. Yang, "High-isolation 3.5 GHz eight-antenna MIMO array using balanced open-slot antenna element for 5G smartphones," *IEEE Trans. Antennas Propag.*, vol. 67, no. 6, pp. 3820–3830, Jun. 2019.

[7] J. Li, X. Zhang, Z. Wang, X. Chen, J. Chen, Y. Li, and A. Zhang, "Dual-band eight-antenna array design for MIMO applications in 5G mobile terminals," *IEEE Access*, vol. 7, pp. 71636–71644, 2019.

[8] A. A. Al-Hadi, J. Ilvonen, R. Valkonen, and V. Viikari, "Eight-element antenna array for diversity and MIMO mobile terminal in LTE 3500 MHz band," *Microw. Opt. Technol. Lett.*, vol. 56, no. 6, pp. 1323–1327, Jun. 2014.

[9] K. L. Wong, J.-Y. Lu, L.-Y. Chen, W.-Y. Li, and Y.-L. Ban, "8-antenna and 16-antenna arrays using the quad-antenna linear array as a building block for the 3.5-GHz LTE MIMO operation in the smartphone," *Microw. Opt. Technol. Lett.*, vol. 58, no. 1, pp. 174–181, Jan. 2016.

[10] M.-Y. Li, Y.-L. Ban, Z.-Q. Xu, G. Wu, C.-Y.-D. Sim, K. Kang, and Z.-F. Yu, "Eight-port orthogonally dual-polarized antenna array for 5G smartphone applications," *IEEE Trans. Antennas Propag.*, vol. 64, no. 9, pp. 3820–3830, Sep. 2016.

[11] Z. Qin, G.-Y. Wen, M. Zhang, and J. Wang, "Printed eight-element MIMO system for compact and thin 5G mobile handest," *Electron. Lett.*, vol. 52, no. 6, pp. 416–418, Mar. 2016.

[12] K.-L. Wong, C.-Y. Tsai, and J.-Y. Lu, "Two asymmetrically mirrored gap-coupled loop antennas as a compact building block for eight-antenna MIMO array in the future smartphone," *IEEE Trans. Antennas Propag.*, vol. 65, no. 4, pp. 1765–1778, Apr. 2017.

[13] Y.-L. Ban, C. Li, C.-Y.-D. Sim, G. Wu, and K.-L. Wong, "4G/5G multiple antennas for future multi-mode smartphone applications," *IEEE Access*, vol. 4, pp. 2981–2988, 2016.

[14] H. Zou, Y. Li, C.-Y.-D. Sim, and G. Yang, "Design of 8 × 8 dual-band MIMO antenna array for 5G smartphone applications," *Int. J. RF Microw. Comput.-Aided Eng.*, vol. 28, no. 9, p. e21420, 2018.

[15] H. S. Aziz and D. K. Naji, "Printed 5G MIMO antenna arrays in smartphone handset for LTE bands 42/43/46 applications," *Prog. Electromagn. Res.*, vol. 90, pp. 167–184, Mar. 2020.

[16] W.-J. Lu and L. Zhu, "Wideband stub-loaded slotline antennas under multi-mode resonance operation," *IEEE Trans. Antennas Propag.*, vol. 63, no. 2, pp. 818–823, Feb. 2015.

[17] S. Zhang, A. A. Glazunov, Z. Ying, and S. He, "Reduction of the envelope correlation coefficient with improved total efficiency for mobile LTE MIMO antenna arrays: Mutual scattering mode," *IEEE Trans. Antennas Propag.*, vol. 61, no. 6, pp. 3280–3291, Jun. 2013.

[18] M. S. Sharawi, "Printed multi-band MIMO antenna systems and their performance metrics [wireless corner]," *IEEE Antennas Propag. Mag.*, vol. 55, no. 5, pp. 218–232, Oct. 2013.

[19] M. P. Karaboikis, V. C. Papamichael, G. F. Tsachtsiris, C. F. Soras, and V. T. Makios, "Integrating compact printed antennas onto small diversity/MIMO terminals," *IEEE Trans. Antennas Progag.*, vol. 56, no. 7, pp. 2067–2078, Jul. 2008.

[20] J. L. Guo, L. Cui, C. Li, and B. H. Sun, "Side-edge frame printed eight-port dual-band antenna array for 5G smartphone applications," *IEEE Trans. Antennas Propag.*, vol. 66, no. 12, pp. 7412–7417, Dec. 2018.

[21] Y. Li, C.-Y.-D. Sim, Y. Luo, and G. Yang, "Metal-frame-integrated eight-element multiple-input multiple-output antenna array in the long term evolution bands 41/42/43 for fifth generation smartphones," *Int. J. RF Microw. Comput.-Aided Eng.*, vol. 29, no. 1, Jan. 2019, Art. no. e21495.

[22] H. Wang, R. Zhang, Y. Luo, and G. Yang, "Compact eight-element antenna array for triple-band MIMO operation in 5G mobile terminals," *IEEE Access*, vol. 8, pp. 19433–19449, 2020.

[23] Y. Li, C.-Y.-D. Sim, Y. Luo, and G. Yang, "12-port 5G massive MIMO antenna array in sub-6 GHz mobile handset for LTE bands 42/43/46 applications," *IEEE Access*, vol. 6, pp. 344–354, Oct. 2017.

[24] N. Jaglan, S. D. Gupta, and M. S. Sharawi, "18 element massive MIMO/diversity 5G smartphones antenna design for sub-6 GHz LTE bands 42/43 applications," *IEEE Open J. Antennas Propag.*, vol. 2, pp. 533–545, 2021.

[25] J. Huang, G. Dong, J. Cai, H. Li, and G. Liu, "A quad-port dual-band MIMO antenna array for 5G smartphone applications," *Electronics*, vol. 10, no. 5, p. 542, Feb. 2021.

[26] J. Huang, G. Dong, Q. Cai, Z. Chen, L. Li, and G. Liu, "Dual-band MIMO antenna for 5G/WLAN mobile terminals," *Micromachines*, vol. 12, no. 5, p. 489, Apr. 2021.

[27] D. Serghiou, M. Khalily, V. Singh, A. Araghi, and R. Tafazolli, "Sub-6 GHz dual-band 8 × 8 MIMO antenna for 5G smartphones," *IEEE Antennas Wireless Propag. Lett.*, vol. 19, no. 9, pp. 1546–1550, Sep. 2020.

[28] L. Cui, J. Guo, Y. Liu, and C.-Y.-D. Sim, "An 8-element dual-band MIMO antenna with decoupling stub for 5G smartphone applications," *IEEE Antennas Wireless Propag. Lett.*, vol. 18, no. 10, pp. 2095–2099, Oct. 2019.

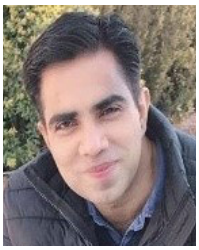

NAVEEN JAGLAN (Member, IEEE) was born in 1989. He received the B.Tech. (Hons.) and M.Tech. (Hons.) degrees in electronics and communication engineering from Kurukshetra University, Kurukshetra, India, in 2009 and 2011, respectively, and the Ph.D. degree in design and development of microstrip antennas integrated with electromagnetic band gap structures from the Jaypee Institute of Information Technology, Noida, Uttar Pradesh, India, in June 2017. He has authored/coauthored several research articles in referred international journals and conferences. His research interests include microwave communications, 5G antenna design, planar and conformal microstrip antennas, including array mutual coupling, artificial materials (metamorphic, metamaterials), EBG, PBG, FSS, DGS, novel antennas, UWB antennas, MIMO systems, numerical methods in electromagnetic, composite right/left handed (CRLH) transmissions, and high-k dielectrics. His skills include modeling of antenna and RF circuits with Ansoft HFSS/CST Microwave Studio/ADS Momentum, measurements using vector network analyzer and anechoic chamber.

SAMIR DEV GUPTA received the B.E. degree in electronics from Bangalore University (University Visvesvaraya College of Engineering, Bengaluru), the M.Tech. degree in electrical engineering from IIT Madras, the M.Sc. degree in defence studies from Madras University, and the Ph.D. degree from JIIT, Noida. He is currently designated as the Director and an Academic Head of the Jaypee University of Information Technology (JUIT), Solan, Waknaghat, Himachal Pradesh, India. He has over three and a half decades of work experience in the areas of avionics, communication, radar systems, and teaching at UG and PG level. His teaching career spans over 22 years and 6 months includes in addition to teaching at JIIT. Since December 2002, he has been teaching at the Institute of Armament Technology, Pune University. He is also with the Defence Institute of Advanced Technology (Deemed University) for PG programs and training and development needs of Indian Air Force (IAF) and Defence Research & Development Organization (DRDO), Air Force Technical College (AFTC), Bengaluru where graduate engineers from IIT's, NIT's, and Indian and foreign universities undergo aeronautical engineering (electronics) course for about 18 months prior joining Technical Officers' Branch, IAF, and Advanced Stage Trade Training Wing at Guided Weapon Training Institute, Baroda. He was also a Recognized Postgraduate Teacher in microwave communication with Pune University. His research interest includes conformal microstrip patch antenna for aircraft systems. His publications in refereed journals and conferences are well cited. His previous assignments includes, the Deputy Director at Air Headquarters and were involved in planning, coordinating and directing maintenance, modification of aircraft and helicopter systems, modifications and induction of advance electronic systems into IAF, a Commanding Officer of an 8-GHz LOS Microwave Communication Unit, a Senior Engineer looking after maintenance of airfield navigation aids, techno-logistic management of ground-based communication equipment as an Aeronautical Engineering (Electronics) Branch Officer of the IAF, and a Chairman Communication Advisory Committee at IAT Pune. He is qualified for first and second line servicing of Mirage-2000 aircraft. His work experience on mirage mission simulator and fly by wire systems of Mirage-2000 aircraft. He led and supervised highly qualified and skilled engineering officers and technicians of the IAF in maintenance and operation of missile, radar, and communication systems. He is experienced in management of resources to achieve time bound targets and objectives viz. successfully implemented contract with international and national agencies for induction of unmanned aerial vehicle, portable laser designating systems and up gradation of aircraft simulators for the IAF.

BINOD KUMAR KANAUJIA (Senior Member, IEEE) received the B.Tech. degree in electronics engineering from Kamla Nehru Institute of Technology, Sultanpur, India, in 1994, and the M.Tech. and Ph.D. degrees from the Department of Electronics Engineering, IIT Banaras Hindu University, Varanasi, India, in 1998 and 2004, respectively. He is currently a Professor with the School of Computational and Integrative Sciences, Jawaharlal Nehru University, New Delhi, India. He had successfully executed five research projects sponsored by several agencies of the Government of India, such as DRDO, DST, AICTE, and ISRO. He has been credited to publish more than 250 research articles with more than 3500 citations and H-index of 27 in several peer-reviewed journals and conferences. He had supervised 50 M.Tech. and 24 Ph.D. scholars in the field of RF and microwave engineering. He is also a member of several academic and professional bodies, such as the Institution of Engineers, India, the Indian Society for Technical Education, and the Institute of Electronics and Telecommunication Engineers of India. He is also on the editorial board of several international journals.

MOHAMMAD S. SHARAWI (Senior Member, IEEE) was with King Fahd University of Petroleum and Minerals (KFUPM), Saudi Arabia, from 2009 to 2018. He founded and directed the Antennas and Microwave Structure Design Laboratory (AMSDL), KFUPM. He was a Visiting Professor with the Intelligent Radio (iRadio) Laboratory, Electrical Engineering Department, University of Calgary, Calgary, AB, Canada, in fall 2014. He was a Visiting Research Professor with Oakland University, in summer 2013. He is currently a Professor of electrical engineering with Polytechnique Montréal, Montréal, QC, Canada. He is also a member of the Poly-Grames Research Center, Polytechnique. He has more than 300 articles published in refereed journals and international conferences, ten book chapters, one single authored book entitled *Printed MIMO Antenna Engineering* (Artech House, 2014) and the Lead Author of the recent book *Design and Applications of Active Integrated Antennas* (Artech house, 2018). He has 25 issued and 12 pending patents in the U.S. Patent Office. His research interests include multiband printed multiple-input-multiple-output (MIMO) antenna systems, reconfigurable and active integrated antennas, applied electromagnetics, millimeter-wave MIMO antennas, and integrated 4G/5G antennas for wireless handsets and access points. He is serving as the Associate Editor for the IEEE Antennas and Wireless Propagation Letters (AWPL) and *IET Microwaves, Antennas and Propagation* (MAP), and an Area Editor for *Microwave and Optical Technology Letters* (MOP) (Wiley). He is the Specialty Editor of the newly launched *Frontiers Journal on Communications and Networking*, the System and Test-Bed Design Section. He served on the technical and organizational program committees of several international conferences, such as EuCAP, APS, IMWS-5G, APCAP, iWAT, and among many others.